HiSST: International Conference on
High-Speed Vehicle Science Technology

26–29 November 2018, Moscow, Russia

Soft-objects based procedure for Thermal Protection System Modelling of Reusable Launch Vehicles

A. Aprovitola[1], L. Iuspa[2], C. Rainone[3], A. Viviani[4]

Abstract

The present paper deals with a modeling procedure of a thermal protection system designed for a conceptual Reusable Launch Vehicle. A novel parametric model based on a scalar field created by a set of soft object primitives, is used to assign an almost arbitrary seamless distribution of insulating materials over the vehicle surface. Macro-aggregates of soft objects are created using suitable geometric supports allowing a distribution of coating materials using a limited number of parameters. Applications to different conceptual vehicle configurations of an assigned thickness map, and materials layout show the flexibility of the model.

Keywords: Hypersonic Vehicles, Thermal Protection System, Soft Objects

1. Introduction

Currently a number of projects related to the development of Reusable Launch Vehicles (RLV) both single-stage-to-orbit (SSTO), and two-stage-to-orbit (TSTO), are ongoing. This trend relates to objectives of future space missions that demand to improve vehicles operability, reducing at the same time flight costs of putting payload into orbit. Several preliminary studies/experiments related to this design scenario have been carried on. European Space Agency developed two demonstrators: the EXPERT (European eXPErimental Re-entry Test-bed) program, and the Intermediate eXperimental Vehicle (IXV) which performed an atmospheric lifting re-entry from orbital speed [1]. Besides, an unmanned lifting body developed by Boeing X-37B, has been put in orbit by an Atlas-5 rocket, and performed a successful lifting-guided re-entry . Furthermore, a growing demand for space tourism has emerged also in recent years [2]; therefore, a great deal of research effort has been put to design RLV as blended wing-bodies also allowing a conventional, and more comfortable landing on runways. Main requirements currently considered for RLV design are: i) to perform very low-g (nearly 1.5 g) reentry; ii) to adopt a light-weight (passive), fully reusable thermal protection system to withstand several flights without any replacement; iii) to provide vehicle autonomy to land at a predefined locations for crew rescue [3], [4]. In order to fulfill all those requirements, the duration of re-entry flight increases, and consequently the integrated heat load absorbed by the structure [3].

The above consideration incidentally demands a trade-off among several non linear conflicting design objectives, also satisfying a number of constraints functions. As an example, the design of the Thermal Protection System (TPS) of an RLV performing a sub-orbital lifting re-entry, requires a mandatory compromise between the maximum allowed peak heating, and the integrated heat load. This requirement may conflict with the adoption of a fully reusable TPS, either limiting the choice of material category or penalizing the total mass. In preliminary design practice, thousand of design configurations are tipically evaluated by an optimization algorithm to find the best fit [5]- [10]. Therefore, a preliminary appraisal of vehicle performances is commonly performed using high-efficiency, low-order fidelity methods, that give a support to a multidisciplinary analysis performed with a computational effort which fit the typical

[1]Università della Campania "L. Vanvitelli", andrea.aprovitola@unicampania.it
[2]Università della Campania "L. Vanvitelli", luigi.iuspa@unicampania.it
[3]Università della Campania "L. Vanvitelli", cinzia.rainone@unicampania.it
[4]Università della Campania "L. Vanvitelli", antonio.viviani@unicampania.it

timeline of the conceptual design phase [11]. In current studies TPS sizing, is performed using several simplified assumptions, carrying out a one-dimensional heat conduction analysis with panel thickness modeled using stackups of different materials [4]. The aerothermal environment is a basic design criterion for either TPS sizing and choice of materials [12, 13]. Several works dealing with TPS sizing have been published in literature. Lobbia [8] determined the sizing of a TPS in the framework of a multi-disciplinary optimization. Material densities, and maximum reuse temperature were computed. TPS mass was estimated assuming the category of materials used for the space Shuttle and thickness distribution assigned on a review of HL-20 materials for each component. Trajectory-based TPS sizing has been proposed by Olynick [13] for a winged vehicle concept. The heating peak was determined considering an X-33 trajectory, discretized in a number of fixed waypoints. The resulting aero-thermal database was used as an input for a one-dimensional conduction analysis, and several one-dimensional stackups of different materials representative of TPS were consequently sized. Bradford et al. [14] developed an engineering software tool for aeroheating analysis and TPS sizing. The tool is applicable in the conceptual design phase for reusable, non-ablative thermal protection systems. The thermal model was based on a one-dimensional analysis, and TPS was modeled considering a stackup of ten different material layers. Mazzaracchio [15] proposed a method to perform the sizing of a TPS depending on the locations of ablative, and reusable zone on a TPS considering the coupling between trajectory, and heat shield. Multidisciplinary analysis, integrating a procedural NURBS-based shape representation, is adopted for a preliminary design [3]. NURBS parameterization, allows a simple control over the aerodynamic shape using a limited number of sensitive design parameters acting as geometrical modifiers. However, derivation of a unique parameterization to describe the overall changes of geometry resulting from a shape optimization is not always possible, and several surfaces are used to parameterize different parts of the geometry. Implicit surfaces are a powerful and alternative tool for creating shapes due to their smooth blending properties enabling creation of arbitrary shape. In the present work, a soft object derived representation for TPS thickness and material attribution, is introduced. According to the legacy formulation of this technique, originally developed in Computer Graphics for the rendering of complex organic shapes [16], three-dimensional object surfaces are (implicitly) obtained by defining a set of source points (or even more complex varieties) irradiating a potential field that is subsequently tracked according to an assigned iso-surface. Following a quite different paradigm developed in [17], the full potential field irradiated by a set of by-dimensional soft objects is congruently mapped on a discretized RLV shape. The methodology is able to create arbitrary TPS distributions seamlessly increasing the thickness where critical heat loads are experienced, and dropping out elsewhere. A similar, slightly modified procedure is also applied to create an arbitrary binary map of different TPS materials that may be operated independently (or syncronized) with the thickness distribution. The present formulation is formalized in the framework of a parametric model which exploits simple variations of parameters to perform the soft object mapping over discretized surface. Applications of the developed procedure to different arbitrary vehicle shape shows the flexibility of the method.

2. Soft Objects definition

Soft objects constitute a modeling technique which typically represents a domain using a scalar field, namely a field function F, defined over a three-dimensional space. An implicit surface S defined as:

$$S = \{\mathbf{x} \in \mathbb{R}^3 | F(\mathbf{x}) = T) \tag{1}$$

i.e. an iso-surface S of the field function F specified by the threshold T, represents an object instance using a raster conversion algorithm. Soft objects modeling, overcomes the drawback given by the parametric surfaces i.e. they automatically allows a self blending between different primitives. Therefore, complex shapes can be modeled defining $n \geq 1$ potential fields f_i, with origin in points $\mathbf{x}_i$, and the blending among them is formally accounted by the algebraic summation of their potential fields f_i [18]:

$$F(d) = \sum_{i=1}^{n} f_i(d_i) \tag{2}$$

A commonly adopted notation

$$F_i(d) = f_i \circ d_i \tag{3}$$

composes the distance metric d_i (which determines the shape of the objects associated to the keypoints $\mathbf{x}_i$), with the field function f_i, being $\mathbf{x}$ is the point of space in which the function is evaluated:

$$d_i = \frac{||\mathbf{x} - \mathbf{x}_i||_k}{r_i} \tag{4}$$

A more powerful representation used in soft object modeling is based on morphological skeleton that synthesizes the morphological properties of a given domain. A skeleton S_k can be defined as a basic geometric entity (such as points, segments, and plain closed domains) around which more complex shapes can be created once the distance function is provided. The simplest soft object was introduced by Blinn that originally proposed the "blobby molecule", an isotropically decaying Gaussian function modulated in strength, and radius [16]:

$$f(d_i) = exp\left(-\frac{{d_i}^2}{2}\right) \tag{5}$$

where d is the Euclidean distance ($k = 2$ in Eq. 4). Blobby molecule, is a soft object defined around a point skeleton, and its field function has an infinite support. This aspect affects the computational effort in a practical implementation, because it has to be evaluated in all points of the space. However, in literature, several finite support potential functions, have been proposed for different modeling purposes. Wyvill et al. [19] developed the following field function:

$$f(d) = \begin{cases} 1 - \frac{22}{9}d^2 + \frac{17}{9}d^4 - \frac{4}{9}d^6 & d^2 < 1 \\ 0 & otherwise \end{cases} \tag{6}$$

Blanc [18] proposed another field function introducing an internal hardness factor p, which tunes the blending between two different blobs. An higher value of p makes a blob stiffer in the blending, while a low hardness factor generates larger rounded shapes [17].

$$f(d) = \begin{cases} 1 - \frac{9d^4}{p+(9/2-4p)d^2} & d^2 \leq 1/4 \\ \\ \frac{(1-d^2)^2}{3/4-p+(3/2+4p)d^2} & 1/4 < d^2 \leq 1 \end{cases} \tag{7}$$

The field function f_i used in the present work has a finite support, and assumes normalized values in the range between 0 and 1 [18]:

$$f(d) = \begin{cases} \frac{1}{2} + \frac{1}{2}\frac{arctan(p-2pd)}{arctanp} & d < 1 \\ 0 & d \geq 1 \end{cases} \tag{8}$$

2.1. Two-dimensional integral soft object for TPS modelling

Two-dimensional soft objects preserve the self-blending property. Figure 1a-b shows the support, and the strength field respectively created superposing n=6 discrete point source blobs with radius r, with origins in keypoints x_i. If $\delta_e < 2r$ two or more blobs superposes, and the strength of the potential field is obtained summing up the strengths of each blob (see Figure 1b). A set of n blobs represents a too complex entity if used to model a parametric variation of shape (a single blob is characterized by five independent parameters i.e. scalar coordinates of centers, strength, and radius). Therefore, blobs can be conveniently, and easily arranged in macro-aggregates with key-points placed on a geometric segment (straight or curved) denoted from now as "sticks". The point source blobs, emulates a segment skeleton with the distance function expressed by Eq.4 (see Fig. 1a). However, a simple algebraic summation of potential fields creates a stick support having "bulges". Increasing the number of blobs, the shape of the support becomes more regular, but the strength of the field function diverges. The above drawback is

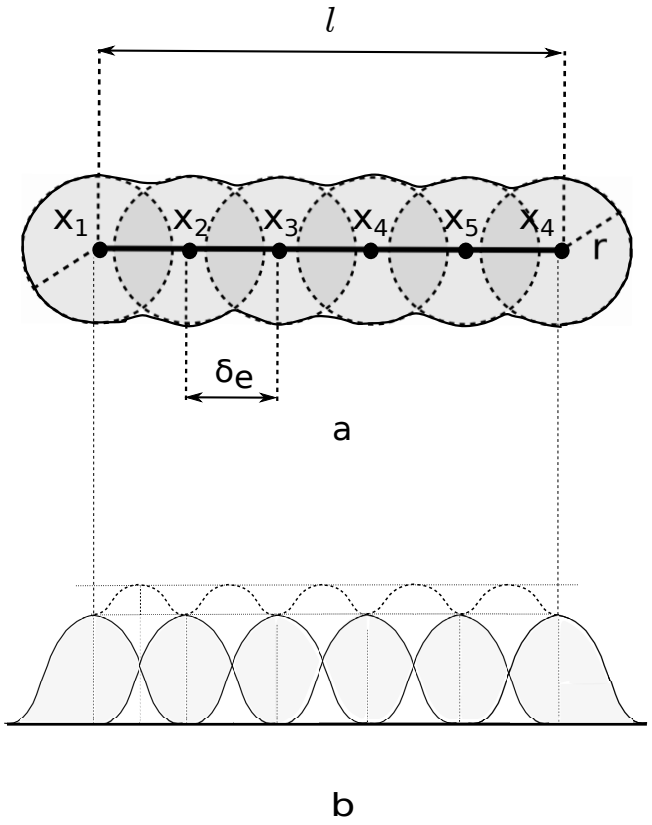

Fig 1. Support (a) and strength field (b) of a stick created by a superposition of $n = 6$ point source blobs.

overcome modifying the definition of potential field given by Eq. 2 with the relation:

$$F_j(P) = \max_{\forall P}(F_{j-1}(P), G_j(P)) \qquad j = 1, \cdots, n_{blobs} \tag{9}$$

Equation 9 where $F_0(P) = 0$, expresses the global potential field $F_j(P)$ irradiated by a set of j blobs at a generic point P of space placed at a distance d from the key-points, as the max between the previous $j-1$ potentials accounted by the assembly layer $F_{j-1}(P)$, and the current potential G_j over the plane disk of radius r:

$$G_j(P) = \begin{cases} f(P) & d < r \\ 0 & otherwise \end{cases} \tag{10}$$

Figure 2A-B shows the support and the strength field of a two-dimensional stick primitive obtained with $n_{blob} = 6$ and 20 respectively computed with Eq. 8. By increasing the number of blob on a stick, the strength of F is still bounded to a maximum unit value. Figure 2C-D shows the same behavior for a tapered primitive having a linear variation of the blob radius along the axis of stick. Therefore, a seamlessly blending of blobs, with a bounded strength is obtained adopting Eq. 9. The procedure proposed here relies on a similar idea to the one developed in [17] to generate self-stiffened structural panels. Specifically, rather than modeling an object tracking an iso-contour of its potential field the full integral field generated by a set of blobs spatially arranged on a two-dimensional grid generates a smoothly varying field.

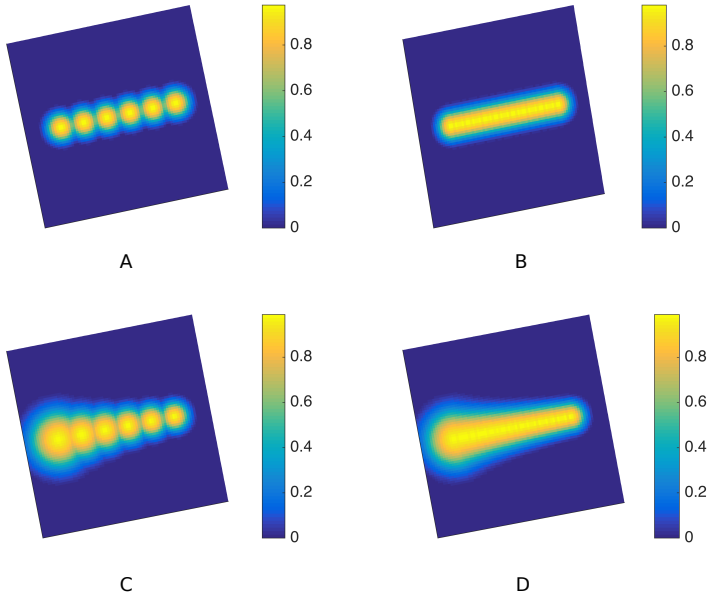

Fig 2. Stick primitives obtained with $n_{blob} = 6$ and 20: constant radius (A-B); variable radius (C-D). The stick support becomes more regular increasing n_{blob}, the strength field remains bounded to unit value.

3. RLV shape modeling

A generic shape of an RLV is represented by a grid formed by a quadrangular and/or by either degenerated triangular panel grid. Grid points are obtained using a proprietary procedure that authors fully detailed in [20], [21]. Without going into details of the shape model, we remark that the mesh arrangement over the RLV surface is obtained with no NURBS support surface: a three-dimensional parametric wireframe is created using cubic rational B-splines, and used to reconstruct computational surface grid. The control parameter, allow a wide range of shape variations to handle different design objectives (thermal or dynamical) for a re-entry mission. Grid topology, is equivalent to a spherical surface with no singularities (open poles), and allows a mapping of the points in UV co-ordinates over an equivalent cylindrical surface. The above considerations ensures a topologically invariant shape.

4. Soft object design of TPS

4.1. Rationale

The modeling procedure for the TPS is defined starting from the definition of a set of soft objects which are represented on the topological map associated with the current morphology of the object, as shown in Fig. 3. Consequently the supports of the sticks are adjusted according to the normalized dimensions relative to this map. The topological map is emulated introducing a two-dimensional grid (from now, denoted as B-grid) having the same topology tree than the vehicle open grid (number of points, panels and connectivity) but unit size. A geometric mapping between the B-grid, and the vehicle grid is established, and elements of B-grid are biunivocally mapped onto corresponding elements of vehicle surface (see Fig. 3). Therefore, each centroid of panels which belong to topological map has the same neighboring points either on the topological or morphological map. Several stick primitives are emulated on B-grid placing a number of n equally-spaced isotropic blobs, with radius r and length l respectively in a normalized units. Stick emulation is performed by overlapping n blobs using the special formulation reported in [17] that ensures a convergent envelope of the finite support, and a limited value of the blob strength. An exemplificative spatial distribution of sticks on the B-grid is shown in Fig. 3. Position and orientation of each stick is determined by assigning coordinates of centers C_i, and precession angles θ_i

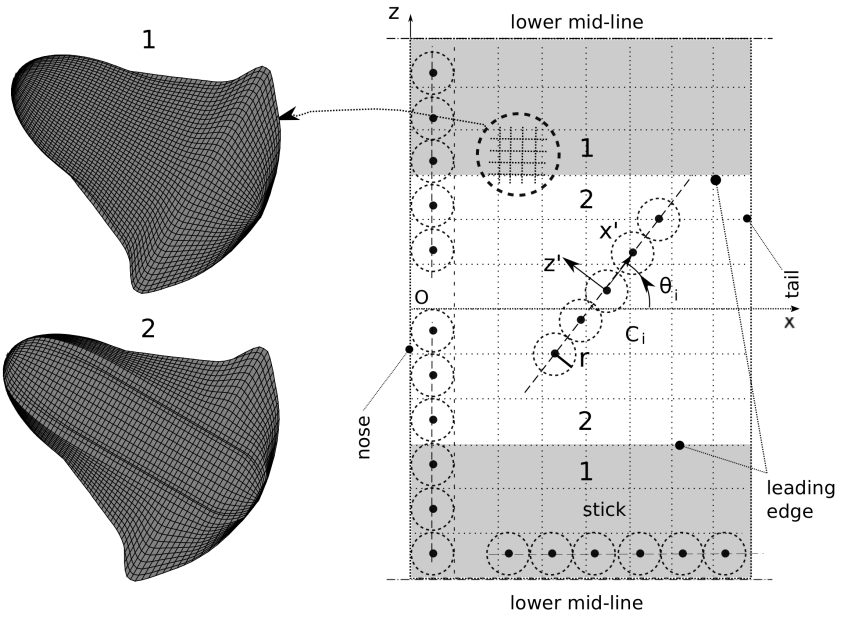

Fig 3. Morphological (left) vs topological map (right).

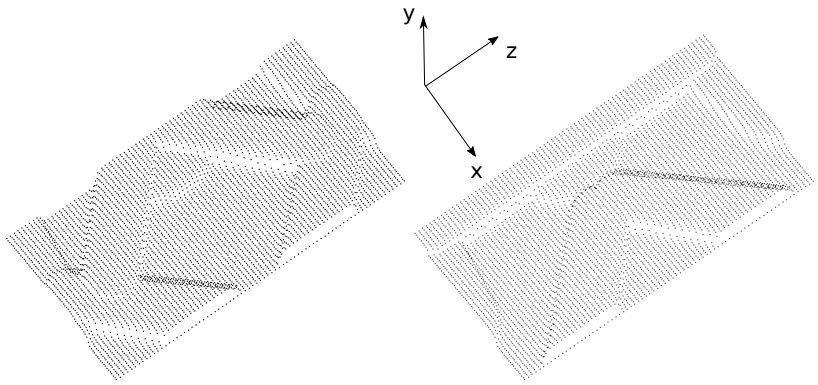

Fig 4. Arbitrary sticks distribution created over the topological map.

respectively, with respect to a Cartesian frame of reference Oxz oriented as in Fig. 3. Therefore, a generic distribution of sticks created on vehicle grid is equally mapped on the vehicle surface whatever is the morphological map considered. In the present case, gray colored regions (1) denote points of the B-grid mapped on the windward side of RLV shape (see Fig. 3), while white regions (2) relates to leeward regions of the vehicle. Regions of vehicle surface mainly subjected to heating peaks during the re-entry maneuver are: i) nose; ii) leading edge, and iii) tail. The global potential field generated by the sticks onto the B-grid is adjusted in a suitable dimensional scale, and subsequently mapped on the mesh panels of the vehicle surface grid to obtain an easy and powerful control of the thickness distribution. The proposed methodology is able to create virtually arbitrary TPS distributions, and can be easily tuned up to locally increase the thickness where critical heat loads are expected, and dropping out elsewhere. A similar, slightly modified procedure is also applied to create an arbitrary binary map distribution of different TPS materials that may be operated independently of the thickness distribution. Figure 4 shows an arbitrary distribution of sticks primitives (not suitable for application purposes) created over the topological map. The resulting potential field created by the superposition of sticks modulates y-coordinate of grid points as shown in Fig. 4.

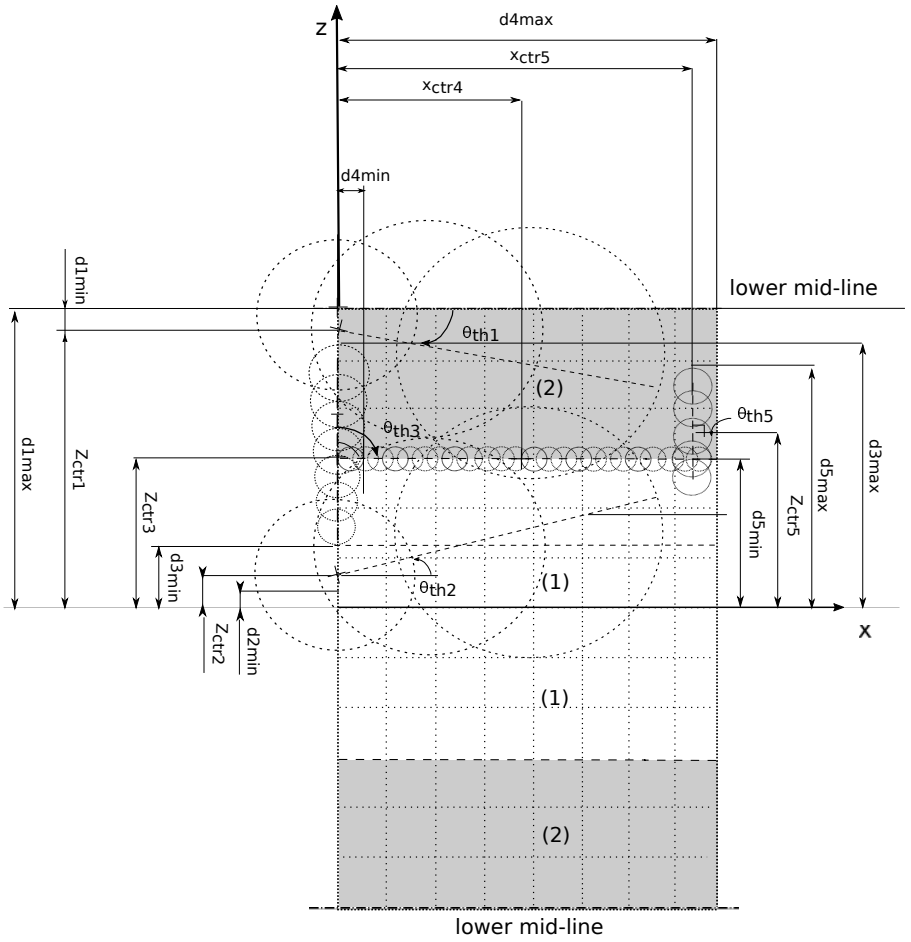

Fig 5. Arbitrary stick distribution with a longitudinal gradient onto B-grid adopted for thermal protection system modeling.

5. Parametric model of Thermal Protection System

5.1. Thickness modeling

As demonstrative example, a parametric representation of thermal protection system is obtained using a limited set of sticks primitive ($n_{stick} = 5$), oriented as shown in Fig. 5. Skin sticks characterized by a large radius and limited strength are spread over the skin surface in longitudinal direction in order to provide a thickness graded baseline. A constant minimum thickness is superposed in all remaining points of B-grid, ensuring a non zero value in any point of the grid. Furthermore, additional parametric sticks, specifically positioned and oriented to affect thickness in critical regions as, nose, leading-edge and trailing edge, complete the support for TPS, and create a rational distribution of insulating material suitable with a re-entry mission. Parametric position of sticks and axis of orientation are defined by assigning centroid coordinates x_c, z_c and angle θ_{th}, measured with respect to the system of reference reported in Fig. 5. Length (l), and strength (th) is expressed with the parametric relations:

$$\begin{cases} x_{c,\{q=1,2,3,4,5\}} & = \{0,0,0,1,1\} \\ z_{c,\{q=1,\dots,5\}} & = d_{q_{min}} + st_q \cdot (d_{q_{max}} - d_{q_{min}}) \\ l_{\{q=1,\dots,5\}} & = lt_q \cdot d_{q_{max}} \\ th_1 & = th'_{min} + pt_1 \cdot (th'_{max} - th'_{min}) \\ th_{\{q=2,\dots,5\}} & = th''_{min} + pt_q \cdot (th''_{max} - th''_{min}) \end{cases} \tag{11}$$

Skin ($q = 1,2$), and nose sticks ($q = 3$) have a tapered support obtained imposing a linear variation of point source blob radius. Conversely, a constant radius is adopted for the leading-edge ($q = 4$), and trailing-edge ($q = 5$) sticks.

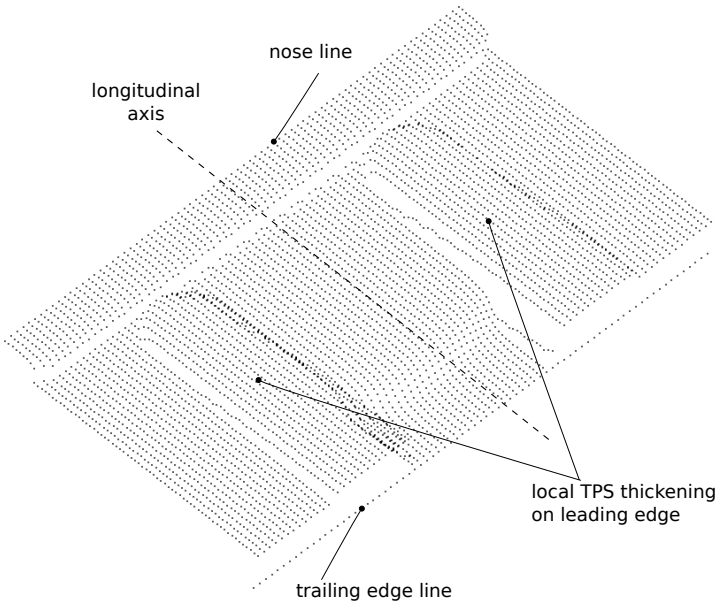

Fig 6. Topological map created to represent TPS thickness on different RLV configurations.

5.2. Material modeling

A similar but completely independent stick-based parameterization, has been also defined to model a dynamic distribution map of different insulating materials, denoted here generically as material 1 and material 2 represented with red and blue color respectively. We assume, that material 1 outperform material 2. Therefore, material 1 is adopted on the nose, leading-edge, and trailing-edge respectively. The parametric equations which describes material assignments are:

$$\begin{cases} mx_{c,\{q=1,2,3,4,5\}} & = \{0,0,0,1,1\} \\ mz_{c,\{q=1,\dots,5\}} & = d_{q_{min}} + mt_q \cdot (d_{q_{max}} - d_{q_{min}}) \\ ml_{\{q=1,\dots,5\}} & = mlt_q \cdot d_{q_{max}} \\ mth_1 & = th^{'}_{min} + mpt_1 \cdot (th^{'}_{max} - th^{'}_{min}) \\ mth_{\{q=2,\dots,5\}} & = th^{''}_{min} + mpt_q \cdot (th^{''}_{max} - th^{''}_{min}) \end{cases} \tag{12}$$

with normalized parameters reported in Table 1.

6. TPS modeling capabilities

The previously introduced modeling procedure has been applied on a conceptual RLV shape created with the model described in Sec 4 and detailed in [20], [21]. Figure 6 shows a topological map obtained for an arbitrarily chosen distribution of stick primitives. A local thickness is assigned on the nose, the leading edge, and the trailing edge. The topological map shown in Fig. 6, creates a morphologically adaptive TPS on two RLV shapes with different dimensions: (RLV-1) with length $l_{tot} = 9.8$ m, wingspan $w_s = 5.6$ m, cabin height $h = 1.6$ m, and (RLV-2) with length $l_{tot} = 15$ m, wingspan $w_s = 9.2$ m, cabin height $h = 2$ m. The parameters characterizing the distribution of thickness, and of the materials are reported in Table 1. Figures 7a-b shows the application of TPS modeling over the first configuration (RLV-1), on leeward (a) and windward (b) surface respectively. Different colors denotes different values

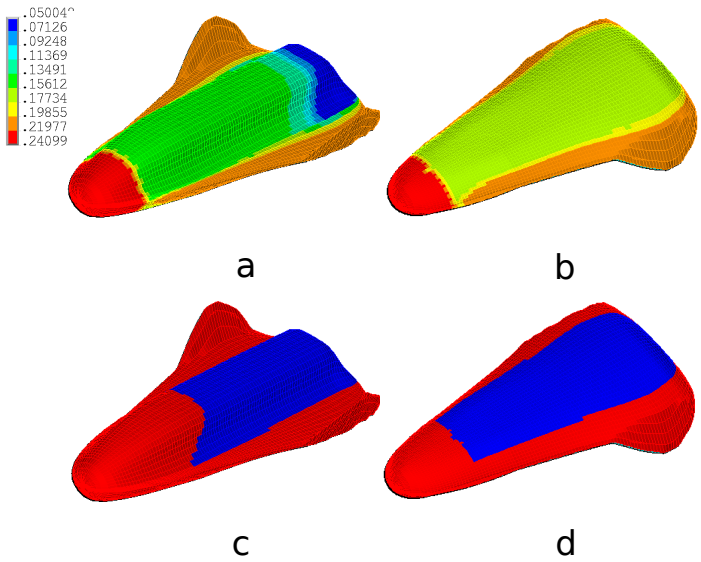

Fig 7. Example of thickness and material distribution over RLV configuration (RLV-1): a-b thickness modulation [m]; c-d two material map (red/blue color indicates material 1/2 respectively).

Parameter	Value	Parameter	Value
st_1, ad	0	mt_1, ad	1
st_2, ad	0.01	mt_2, ad	0.01
st_3, ad	0.05	mt_3, ad	0.05
st_4, ad	1	mt_4, ad	1
st_5, ad	0.8	mt_5, ad	0.8
lt_1, ad	1	mlt_1, ad	1
lt_2, ad	0.1	mlt_2, ad	0.1
lt_3, ad	1	mlt_3, ad	1
lt_4, ad	1	mlt_4, ad	1.2
lt_5, ad	1	mlt_5, ad	1
p_{t_1}, ad	1	mpt_1, ad	1
p_{t_2}, ad	0.2	mpt_2, ad	1
p_{t_3}, ad	0.5	mpt_3, ad	1
p_{t_4}, ad	0.2	mpt_4, ad	1
p_{t_5}, ad	0.6	mpt_5, ad	1
d_{1min}, ad	0.5	d_{1max}, ad	1
d_{2min}, ad	0.01	d_{2max}, ad	0.3
d_{3min}, ad	0.09	d_{3max}, ad	1
d_{4min}, ad	0.1	d_{4max}, ad	0.5
d_{5min}, ad	0.02	d_{5max}, ad	0.5
th'_{min}, ad	0.07	th'_{max}, ad	0.12
th''_{min}, ad	0.132	th''_{max}, ad	0.25

Table 1. Parameters adopted in the modeling of TPS configurations of Fig. 7 and Fig. 8.

of thickness, and are represented in a dimensional scale. It can be observed that the thickness map can be easily tuned up for best covering of regions where maximum heat loads occurs (i.e. the nose and leading edge). Figure 7, shows the capability to create arbitrary seameless thickness distribution up to the value of the baseline thickness which has been arbitrarily set equal to $th_{min} = 0.05$ m (denoted in blue color). This correspond to a region of the leeward surface not covered by the skin stick. Figures 7c-d shows the map of two different insulating material created with Eq. 7. Red colors indicates material 1, which is placed on regions of the vehicle subjected to higher heat loads. Comparisons between Fig. 7a-b

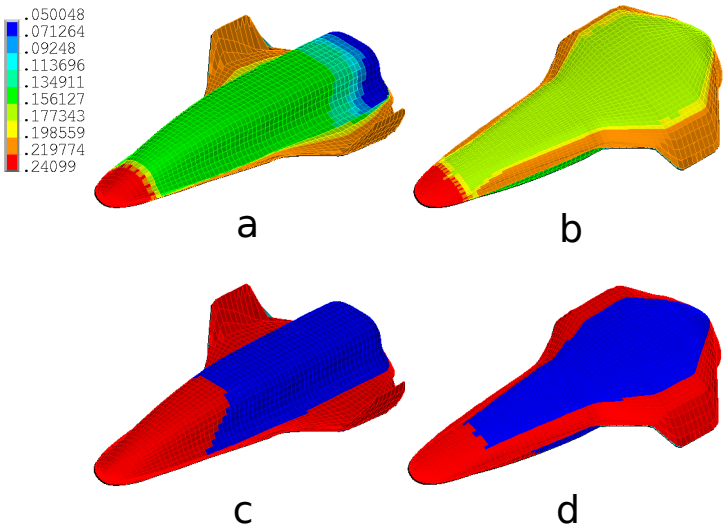

Fig 8. Example of thickness and material distribution over RLV configuration (RLV-2): a-b thickness modulation [m]; c-d two material map (red/blue color indicates material 1/2 respectively).

and Fig.7c-d also exhibits the capability of the model to handle independently both the thickness and material distribution. Finally, Fig. 8a-b, and Fig. 8c-d shows the same blob distribution adopted either for thickness or material modeling applied on a different RLV configuration (RLV-2). The procedure creates, as it was expected, the same TPS distribution both for thickness or materials on two different shapes, and is completely independent by their morphology.

7. Conclusions

In the present paper a special modeling procedure of the thermal protection system designed for a conceptual Reusable Launch Vehicle has been developed. A set of macro-aggregates of point source blobs organized in envelopes of finite supports, and with a bounded strength has been successfully created on the topological map associated to the computational grid. Applications of the modeling procedure to different design configurations, highlighted the sensitivity, and powerful control to radically change the TPS using a limited number of parameters. The promising capabilities of the developed modeling procedure to give support to a multidisciplinary analysis

References

1. Sziroczak, D., Smith, H.: A review of design issues specific to hypersonic flight vehicles. Progress in Aerospace Sciences, 84, 1-28 (2016)

2. DePasquale, D., Charania, A.C., Olds, J.R.: The emerging orbital space tourism industry: New insight into demand and prospect for success. AIAA Paper 2006-7478 (2006)

3. Hirschel, E., Weiland, C.: Selected Aero-thermodynamic Design Problem of Hypersonic Flight Vehicles. Springer-Verlag/AIAA (2009)

4. Dirkx, D., Mooij, E.: Conceptual shape optimization of entry vehicles applied to Capsules and Winged Fuselage Vehicles, Springer aerospace technology, Springer International Publishing Switzerland (2017)

5. Dirkx, D., Mooij, E.: Optimization of entry-vehicle shapes during conceptual design. Acta Astronautica, 94,1, 198-214 (2014)

6. Ridolfi, G., Mooji, E., Dirkx, D., Corpino, S.: Robust Multi-Disciplinary Optimization of Unmanned Entry Capsules. AIAA Paper 2012-5006 (2012)

7. Rowell, R.,F., Braun, R., D.: Multidisciplinary conceptual design optimization of space transportation systems. Journal of Aircraft, 35, No.1, 218-226 (1999)

8. Lobbia, M., A.: Multidisciplinary Design Optimization of Waverider-Derived Crew Reentry Vehicles. Journal of Spacecraft and Rockets, 54, No.1, 233-245 (2017)

9. Foster, N., F., Dulikravic, G., S.: Three-Dimensional Aerodynamic shape optimization using genetic and gradient search algorithms. Journal of Spacecraft and Rockets, 34, No.1, (1997)

10. Zhang, T-t., Wang, Z-g., Huang, W., Yan., L.: Parameterization and optimization of hypersonic-gliding vehicle configurations during conceptual design, Aerospace Science and Technology, 58, 225-234, (2016)

11. Hinman, W., S., Johansen, C., T.: Rapid Prediction of Hypersonic Blunt Body Flows for Parametric Design Studies. Aerospace science and technology, 58, 48-59, (2016)

12. Kumar, S., Mahulikar, S., P.: Design of Thermal Protection System for Reusable Hypersonic Vehicle Using Inverse Approach. Journal of Spacecraft and Rockets, 54, 2, 436-446, (2017)

13. Olynick, D.: Trajectory-Based Thermal Protection System Sizing for an X-33 Winged Vehicle Concept. Journal of Spacecraft and Rockets, 35, 3, 249-256, (1998)

14. Bradford, J., E.: Thermal protection system sizing and selection for RLV using the sentry code. AIAA Paper 2006-4605, (2006)

15. Mazzaracchio, A.: Thermal protection system and trajectory optimization for orbital plane change aeroassisted maneuver. J. Aerospac. Technol. Manag. Sao Jose dos Campos, 5, 1, 49-64, (2013)

16. Blinn, J., F.: A generalization of algebraic surface drawing. ACM Transaction on Graphics, 68, No.3, 123-134, (1982)

17. L. Iuspa: Free topology generation of self-stiffened panels using skeleton-based integral soft objects. Computer & Structures 158, 184-210, (2015)

18. Blanc, C., Schlick, C.: Extended field functions for soft objects. Proc. Implicit Surface'95 (Grenoble, France), 21-32

19. G., Wyvill, C., Pheeters, B., Wyvill: Data structures for soft objects. Visual Computer, 2, 227-234, (1986)

20. Viviani, A., Iuspa, L., Aprovitola, A.: An optimization-based procedure for self-generation of Re-entry Vehicles shape. Aerospace Science and Technology, 68, 123-134, (2017)

21. Viviani, A., Iuspa, L., Aprovitola, A.: Multi-objective optimization for re-entry spacecraft conceptual design using a free-form shape generator. Aerospace Science and Technology, 71, 312-324, (2017)